

Yu, Cao et al.

Article

Field performance evaluation of various crystalline silicon photovoltaic technologies in Pingshan, China

Energy Reports

Provided in Cooperation with:

Elsevier

Suggested Citation: Yu, Cao et al. (2019) : Field performance evaluation of various crystalline silicon photovoltaic technologies in Pingshan, China, Energy Reports, ISSN 2352-4847, Elsevier, Amsterdam, Vol. 5, pp. 525-528, <https://doi.org/10.1016/j.egyr.2019.04.006>

This Version is available at:

<https://hdl.handle.net/10419/243607>

Standard-Nutzungsbedingungen:

Die Dokumente auf EconStor dürfen zu eigenen wissenschaftlichen Zwecken und zum Privatgebrauch gespeichert und kopiert werden.

Sie dürfen die Dokumente nicht für öffentliche oder kommerzielle Zwecke vervielfältigen, öffentlich ausstellen, öffentlich zugänglich machen, vertreiben oder anderweitig nutzen.

Sofern die Verfasser die Dokumente unter Open-Content-Lizenzen (insbesondere CC-Lizenzen) zur Verfügung gestellt haben sollten, gelten abweichend von diesen Nutzungsbedingungen die in der dort genannten Lizenz gewährten Nutzungsrechte.

Terms of use:

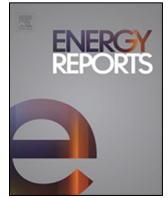
Documents in EconStor may be saved and copied for your personal and scholarly purposes.

You are not to copy documents for public or commercial purposes, to exhibit the documents publicly, to make them publicly available on the internet, or to distribute or otherwise use the documents in public.

If the documents have been made available under an Open Content Licence (especially Creative Commons Licences), you may exercise further usage rights as specified in the indicated licence.



<https://creativecommons.org/licenses/by-nc-nd/4.0/>



Research paper

Field performance evaluation of various crystalline silicon photovoltaic technologies in Pingshan, China

Cao Yu ^{a,b,1}, Jing Chai ^{c,*}, Shuwei Han ^{b,d,1}, Zi Liu ^b, Xiaobo Li ^d, Jianxi Yao ^a

^a The School of Renewable Energy, North China Electric Power University, Beijing 102206, China

^b China Three Gorges New Energy Co., Ltd, Beijing 100053, China

^c National University of Singapore, 7 Engineering Drive 1, Singapore 117574, Singapore

^d China Three Gorges New Energy North China Co., Ltd, Hebei 050051, China



ARTICLE INFO

Article history:

Received 1 February 2019

Received in revised form 5 April 2019

Accepted 11 April 2019

Available online 10 May 2019

Keywords:

Photovoltaics

Crystalline silicon

Field performance

Spectral mismatch

Energy yield

ABSTRACT

The field performance of three different crystalline silicon photovoltaic (PV) module technologies in Pingshan, China (BSk climate based on the Köppen–Geiger climate classification) is analyzed and compared, including p-type multicrystalline silicon (multi-Si), p-type monocrystalline silicon (mono-Si) and n-type mono-Si modules. Both p-type multi-Si and mono-Si solar cells are of the conventional type with back-surface field, whereas the n-type device is of the heterojunction (HET) type. From January 2017 to December 2018, the n-type HET modules showed the best field performance (in terms of kWh/kWp) with an average daily energy yield of 3.9 kWh/kWp. The p-type multi-Si and mono-Si modules performed similarly with an average daily energy yield of 3.7 kWh/kWp (marginally better for multi-Si modules). On-site measurements also showed that the location has a ‘blue-rich’ and ‘red-rich’ spectrum in the summer and winter, respectively. In general, the spectral effect is positive in the summer, and negative in the winter, for all three investigated c-Si PV technologies. Besides, the spectral effect slightly favors the HET technology in the summer, but the opposite is true for mono-Si and multi-Si devices in the winter.

© 2019 The Authors. Published by Elsevier Ltd. This is an open access article under the CC BY-NC-ND license (<http://creativecommons.org/licenses/by-nc-nd/4.0/>).

1. Introduction

The worldwide photovoltaic (PV) deployment is growing rapidly, with nearly 100 GW of PV capacity installed in 2017 (SNAPSHOT, 2018). While several emerging PV concepts (e.g., perovskite solar cells) are attracting huge interest in academia, crystalline silicon (c-Si) wafer-based PV technologies dominated the market with over 90% share in 2017; more specifically, multicrystalline and monocrystalline silicon (multi-Si and mono-Si) modules accounted for 60% and 32% of PV production, respectively (Photovoltaics, 2018). In general, multi-Si wafers are relatively cheaper than their mono-Si counterparts, but PV conversion efficiency is slightly compromised due to additional crystal defects and metal contaminations.

With the rapid growth of PV deployment, it is important to understand their performance under real-world field conditions. PV modules are rated under standard testing conditions with an irradiance of 1000 W/m², the solar spectrum of AM1.5G, and temperature of 25 °C. However, these conditions are rarely encountered

in the real world. Therefore, STC ratings might not necessarily be representative of the field performance. PV modules’ energy production is influenced by various factors in real-world applications (Sharma and Goel, 2017; Shiva Kumar and Sudhakar, 2015; Sharma and Chandel, 2013). For example, the operating cell temperature is significantly higher than the ambient temperature due to the heating from solar irradiation, and thus the power output is reduced (Dubey et al., 2013). In addition, the solar intensity and spectrum are also constantly changing outdoors, resulting in a discrepancy between the projected (based on STC ratings) and the actual power generation (Polo et al., 2017; Alonso-Abella et al., 2014). Other factors such as soiling (Massi Pavan et al., 2011), angle of incidence (Mialhe et al., 1991) and snowing further compromise PV modules’ performance (Andenès et al., 2018). Hence, it is important to investigate the field performance of PV modules for all stakeholders in the PV value chain, considering that hundreds of billions of dollars are being invested every year.

In this study, the real-world field performance of three different c-Si PV module technologies in Pingshan, China (BSk climate based on the Köppen–Geiger climate classification) is evaluated and compared, including p-type multi-Si, p-type mono-Si and n-type mono-Si PV modules. Both p-type multi-Si and mono-Si solar cells are of the conventional type with back-surface field (BSF), whereas the n-type device is of the heterojunction (HET) type.

* Correspondence to: National University of Singapore, 7 Engineering Drive 1, Block E3A, #06-01, Singapore 117574, Singapore.

E-mail address: chaijing@foxmail.com (J. Chai).

¹ These authors contributed equally.



Fig. 1. The tested located at Pingshan, China (38.3°N, 114.0°E) for evaluating PV modules' field performance.

Table 1

Specifications of three types of c-Si PV modules deployed in the testbed, based on the manufacturer's datasheet. All module types have 60 full-size solar cells and are mono-facial modules with a glass/backsheet structure.

Module type	Power (W)	Short-circuit current (A)	Open-circuit voltage (V)	Module power temperature coefficient (%/°C)
Multi-Si	255	8.9	37.5	−0.41
Mono-Si	265	9.2	38.2	−0.41
HET	280	8.7	42.8	−0.29

2. Testbed set-up

The testbed is located at Pingshan, China (38.3°N, 114.0°E) on the back of a hill (see Fig. 1), consisting of multiple PV systems (rack-mounted). Details of the climatic conditions of the test site can be found at [Available \(0000\)](#) (BSk climate based on the Köppen–Geiger climate classification). In this study, three PV systems with similar tilt angles ($\sim 36^\circ$) and orientation (facing south) are analyzed. They are constructed with three different types of c-Si PV modules, i.e., p-type multi-Si BSF, p-type mono-Si BSF and n-type mono-Si HET modules. The specifications of these modules are summarized in Table 1. For all three PV systems, 22 modules (of the same type) are serially connected in a string; multiple strings are then combined and connected to an inverter, which feeds electricity into the grid. These systems have been monitored since January 2017. Production data, module temperature (measured on rear module surfaces) and spectral irradiance (MS-710 from EKO Instruments) are recorded.

3. Results and discussion

3.1. Comparison of multi-Si, mono-Si and HET modules' field performance

Fig. 2 shows the comparison of the daily energy yield of the multi-Si, mono-Si and HET modules from January 2017 to December 2018. It is observed that the HET modules outperformed the multi-Si and mono-Si modules throughout the year (by about 6% on average), with an average daily energy yield of 3.9 kWh/kWp. The superior field performance of the HET modules may be attributed to several factors, such as a lower module power temperature coefficient (see Table 1) and the spectral effect. For example, Fig. 3 demonstrates the temperature effect on PV modules' performance loss in the field. For conventional multi-Si and mono-Si modules, the module output is reduced by up to nearly 14% in the middle of a summer day because of

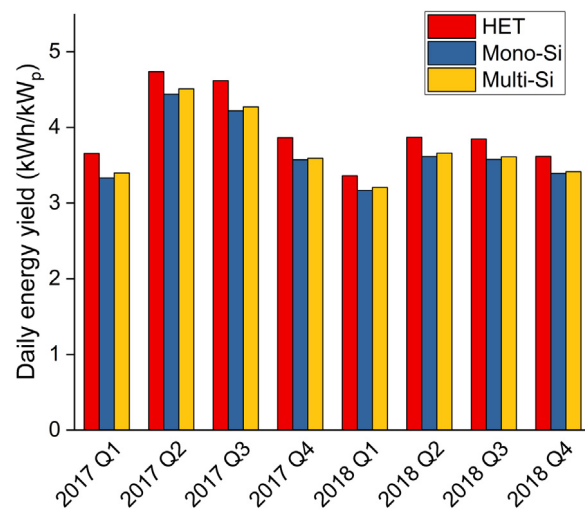


Fig. 2. The daily energy yield of three investigated PV module types from January 2017 to December 2018.

the heat; however, the reduction is significantly lower ($< 10\%$) for HET modules. The higher energy yield from HET technologies compensates for their higher initial cost. Therefore, it is expected that n-type HET technologies will become more competitive and gain more market share in the future. In addition, the multi-Si and mono-Si modules exhibited similar performance (marginally better for multi-Si modules) with an average daily energy yield of 3.7 kWh/kWp. The percentage difference of module energy yield (kWh/kWp) in different periods of the year is also summarized in Table 2, using the multi-Si modules as the reference.

3.2. Effect of the solar spectral distribution

The effect of the solar spectral distribution on the field performance of these three types of c-Si PV modules is also investigated. Fig. 4 shows the solar spectral distribution measured at the testbed on a clear day (around noon time) in the summer and winter, respectively. The AM 1.5 spectrum is also shown as a reference. The average photon energy (i.e., APE) from 350 to 1050 nm is calculated using Eq. (1) (Norton et al., 2015). On a clear day in the summer, the APE value (i.e., 1.89 eV) is slightly higher than that of the AM1.5 standard solar spectrum (i.e., 1.88 eV); hence, it is 'blue-rich'. To the contrary, the solar spectrum in the winter is 'red-rich' (< 1.88 eV). This can also be concluded

Table 2

The percentage difference of module energy yield (kWh/kWp) in difference periods of the year from January 2017 to December 2018, using the multi-Si modules as the reference.

Module type	2017 Q1	2017 Q2	2017 Q3	2017 Q4	2018 Q1	2018 Q2	2018 Q3	2018 Q4
Mono-Si	−2.0%	−1.6%	−1.2%	−0.5%	−1.3%	−1.3%	−1.0%	−0.7%
HET	7.5%	5.0%	8.1%	7.7%	4.8%	5.7%	6.5%	6.0%

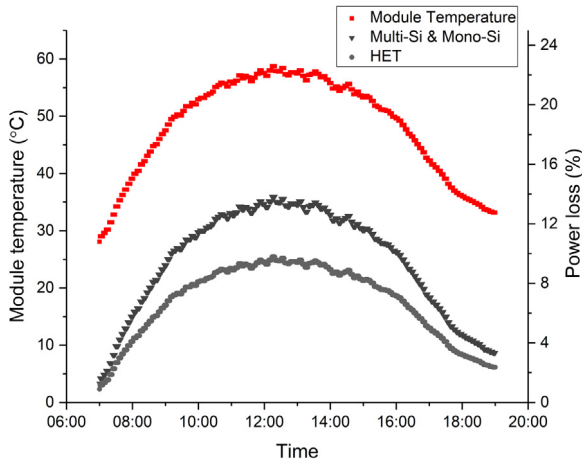


Fig. 3. The effect of operating temperature on PV modules' output. Left y-axis shows the module temperature, and the right y-axis shows the power loss due to temperature effect. The module temperature (plotted in red) is measured on a multi-Si module (on a clear day in summer), and it is assumed that all three module types operate at the same temperature. The power loss (relative to 25 °C) calculated, using the module power temperature coefficient from Table 1.

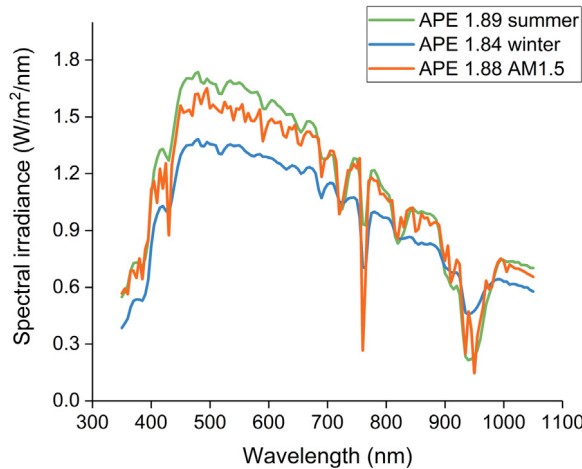


Fig. 4. Solar spectrum measured on a clear day in the summer and winter (at Pingshan, China), respectively. The corresponding APE values are also shown.

from the distribution of the APE values. As shown in Fig. 5, the median of the APE values of July 2017 is larger than 1.88 eV (indicated by the black dash line), whereas the median of the APE values of January 2017 is well below 1.88 eV.

$$APE = \frac{\text{Integrated irradiance}}{\text{Total photon number}} = \frac{\int_{\lambda_1}^{\lambda_2} E(\lambda)d\lambda}{q \int_{\lambda_1}^{\lambda_2} \phi(\lambda)d\lambda} \quad (1)$$

where E is the spectral irradiance; λ is the wavelength; q is the elementary charge; and ϕ is the photon flux density.

The external quantum efficiency (EQE) of these three c-Si PV technologies is also measured. As shown in Fig. 6, the mono-Si and multi-Si modules show higher EQE response than the HET device in the blue spectral region. On the other hand, for

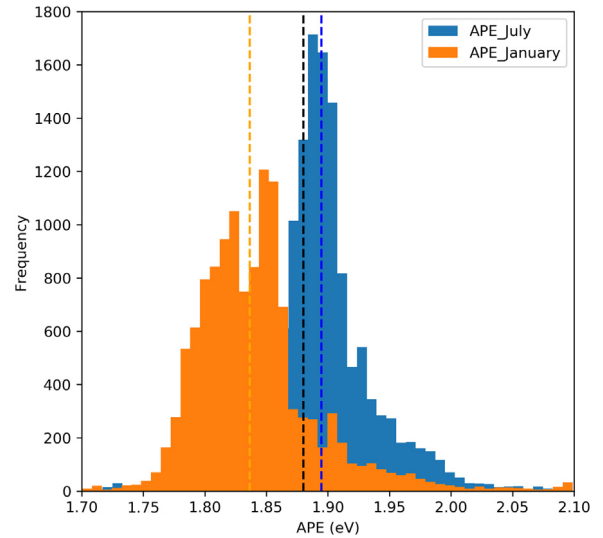


Fig. 5. Distribution of the APE values in January 2017 (orange) and July 2017 (blue) at Pingshan, China. The black dash line represents APE = 1.88 eV, where the orange and blue dash lines represent the median of the APE distribution in January 2017 and July 2017, respectively. (For interpretation of the references to color in this figure legend, the reader is referred to the web version of this article.)

Table 3

Spectral factors for the c-Si PV modules based on the solar spectrum measured on a clear day (around noon time) in the summer and winter at Pingshan, China.

	HET	Mono-Si	Multi-Si
Summer	1.015	1.012	1.011
Winter	0.988	0.990	0.991

wavelengths over 850 nm, the HET module is more effective in converting photons to electrons than the mono-Si and multi-Si devices. The spectral factor (SF) is then calculated for a typical day in the summer and winter to quantify the spectral effect, using Eq. (2) (Pofo et al., 2017; Alonso-Abella et al., 2014; Pérez-López et al., 2007). SF values are often used as an estimation of the relative energetic gain or loss due to the actual spectral differences from the standard conditions for PV devices with values higher than 1 meaning spectral gain and vice versa. The results are shown in Table 3. In general, the spectral effect is positive (about 1% gain) in the summer, and negative (about 1% loss) in the winter, for all three investigated c-Si PV technologies. Furthermore, the spectral effect is slightly in favor of the HET technology in the summer, but the opposite is true for mono-Si and multi-Si devices in the winter.

$$SF = \frac{\int_{\lambda_1}^{\lambda_2} E_{AM1.5G}(\lambda) SR(\lambda)d\lambda \int_{\lambda_1}^{\lambda_2} E(\lambda)d\lambda}{\int_{\lambda_1}^{\lambda_2} E(\lambda)SR(\lambda)d\lambda \int_{\lambda_1}^{\lambda_2} E_{AM1.5G}(\lambda)d\lambda} \quad (2)$$

where $E_{AM1.5G}$ is the spectral irradiance of the AM1.5G spectrum and SR is the spectral response of the PV devices.

4. Conclusion

In this study, the real-world field performance of three different c-Si PV module technologies in Pingshan, China was studied

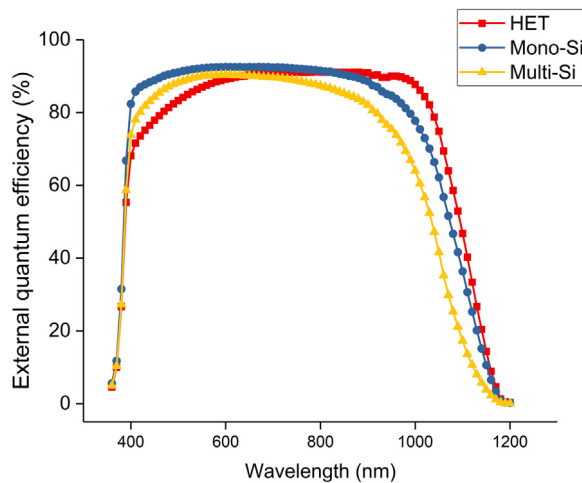


Fig. 6. External quantum efficiency of the three investigated c-Si PV technologies (measured with IVT Solar, PVE-300). Note the bill of materials for the fielded modules and the EQE samples are different, as the purpose is to demonstrate the relative significance of the spectral effect.

and analyzed, including p-type multi-Si BSF, p-type mono-Si BSF and n-type mono-Si HET modules, from January 2017 to December 2018. The HET modules outperformed (in terms of kWh/kWp) the multi-Si and mono-Si modules throughout the year (by about 6% on average). The multi-Si and mono-Si modules performed similarly outdoors with an average daily energy yield of 3.7 kWh/kWp (marginally better for multi-Si modules). One key reason for the superior field performance from HET modules is their lower power temperature coefficient, compared to conventional multi-Si and mono-Si modules. In addition, on-site measurements also showed that the location has a ‘blue-rich’ and ‘red-rich’ spectrum in the summer and winter, respectively. In general, the spectral effect is positive in the summer, and negative in the winter, for all three investigated c-Si PV technologies. Besides, the

spectral effect slightly favors the HET technology in the summer, but the opposite is true for mono-Si and multi-Si devices in the winter.

Acknowledgment

This work was supported by the National University of Singapore and China Three Gorges New Energy Co. Ltd.

References

- Alonso-Abella, M., Chenlo, F., Nofuentes, G., Torres-Ramírez, M., 2014. Analysis of spectral effects on the energy yield of different PV (photovoltaic) technologies: The case of four specific sites. *Energy* 67, 435–443.
- Andenès, E., Jelle, B.P., Ramlo, K., Kolås, T., Selj, J., Foss, S.E., 2018. The influence of snow and ice coverage on the energy generation from photovoltaic solar cells. *Sol. Energy* 159, 318–328.
- Available: <https://en.climate-data.org/asia/china/hebei/平山县-994401/> Accessed on 2019/04/03.
- Dubey, S., Sarvaiya, J.N., Seshadri, B., 2013. Temperature dependent photovoltaic (PV) efficiency and its effect on PV production in the world – a review. *Energy Procedia* 33, 311–321.
- Massi Pavan, A., Mellit, A., De Pieri, D., 2011. The effect of soiling on energy production for large-scale photovoltaic plants. *Sol. Energy* 85 (5), 1128–1136.
- Mialhe, P., Mouhamed, S., Haydar, A., 1991. The solar cell output power dependence on the angle of incident radiation. *Renew. Energy* 1 (3), 519–521.
- Norton, M., Amillo, A.M.G., Galleano, R., 2015. Comparison of solar spectral irradiance measurements using the average photon energy parameter. *Sol. Energy* 120, 337–344.
- Pérez-López, J.J., Fabero, F., Chenlo, F., 2007. Experimental solar spectral irradiance until 2500 nm: results and influence on the PV conversion of different materials. *Prog. Photovolt., Res. Appl.* 15 (4), 303–315.
- Photovoltaics, 2018. Photovoltaics report, Fraunhofer Institute for Solar Energy Systems.
- Polo, J., Alonso-Abella, M., Ruiz-Arias, J.A., Balenzategui, J.L., 2017. Worldwide analysis of spectral factors for seven photovoltaic technologies. *Sol. Energy* 142, 194–203.
- Sharma, V., Chandel, S.S., 2013. Performance and degradation analysis for long term reliability of solar photovoltaic systems: A review. *Renew. Sustain. Energy Rev.* 27, 753–767.
- Sharma, R., Goel, S., 2017. Performance analysis of a 11.2 kwp roof top grid-connected PV system in eastern India. *Energy Rep.* 3, 76–84.
- Shiva Kumar, B., Sudhakar, K., 2015. Performance evaluation of 10 MW grid connected solar photovoltaic power plant in India. *Energy Rep.* 1, 184–192.
- 2018. SNAPSHOT OF GLOBAL PHOTOVOLTAIC MARKETS, IEA PVPS.